Bioorganic & Medicinal Chemistry Letters 25 (2015) 3914–3920

Contents lists available at ScienceDirect

Bioorganic & Medicinal Chemistry Letters

journal homepage: www.elsevier.com/locate/bmcl

Discovery and structure-guided optimization of *tert*-butyl 6-(phenoxymethyl)-3-(trifluoromethyl)benzoates as liver X receptor agonists

Yumi Matsui [a,*], Takahiro Yamaguchi [b], Takanori Yamazaki [b], Masayuki Yoshida [b], Masami Arai [b], Naoki Terasaka [b], Shoko Honzumi [b], Kenji Wakabayashi [a], Shinko Hayashi [b], Daisuke Nakai [b], Hiroyuki Hanzawa [a], Kazuhiko Tamaki [b,*]

[a] Daiichi Sankyo RD Novare Co., Ltd, 1-16-13, Kita-Kasai, Edogawa-ku, Tokyo 134-8630, Japan
[b] R&D Division, Daiichi Sankyo Co., Ltd, 1-2-58 Hiromachi, Shinagawa-ku, Tokyo 140-8710, Japan

ARTICLE INFO

Article history:
Received 31 March 2015
Revised 7 July 2015
Accepted 16 July 2015
Available online 23 July 2015

Keywords:
Liver X receptors
LXR agonists
Atherosclerosis
tert-Butyl benzoate
Structure-based drug design

ABSTRACT

To obtain potent liver X receptor (LXR) agonists, a structure–activity relationship study was performed on a series of *tert*-butyl benzoate analogs. As the crystal structure analysis suggested applicable interactions between the LXR ligand-binding domain and the ligands, two key functional groups were introduced. The introduction of the hydroxyl group on the C6-position of the benzoate part enhanced the agonistic activity in a cell-based assay, and the carboxyl group in terminal improved the pharmacokinetic profile in mice, respectively. The obtained compound **32b** increased blood ABCA1 mRNA expression without plasma TG elevation in both mice and cynomolgus monkeys.

The liver X receptor α and β (LXRα and β) are members of the nuclear hormone receptor superfamily.[1] LXRα is mainly expressed in the liver, adipose tissue, and macrophage, whereas LXRβ is expressed ubiquitously. LXRs regulate lipid metabolism and reverse cholesterol transport by controlling the gene expression of ApoE[2] and ATP-binding cassette transporters A1 and G1 (ABCA1 and ABCG1),[3] which play an important role in cholesterol efflux from adipocyte and macrophage.[4] Various research shows liver X receptors (LXRs) as potential therapeutic targets for atherosclerosis by enhancing the cholesterol efflux promotion from macrophages.[5]

The synthetic LXR agonists, such as T0901317 (**1**) and GW3965 (**2**) (Fig. 1, Table 1), have been described as increasing the ABCA1 expression and reducing atherosclerotic plaque in a LDLR−/− mouse model.[6,7] However, these compounds also increase the plasma and the liver triglyceride (TG) levels by induction of the sterol regulatory element-binding protein-1c (SREBP-1c).[8] SREBP-1c activates the transcription of genes involved in fatty acid biosynthesis, including fatty acid synthase (FAS) and stearoyl CoA desaturase-1 (SCD-1).[9] For therapeutic use, the agonists which have a wide therapeutic window between the induction of ABCA1 and TG elevation are desirable.

A mammalian two-hybrid assay using LXRβ and SRC-1 was developed for a high-throughput screening (HTS), which identified a novel *N*-Boc-indole analog **3** as a ligand to LXRs (Fig. 2). Separately from the chemical modification of **3** with the *N*-Boc-indole core intact, early chemical modification of the indole ring in **3** led to **4**, a potent binder to LXRs (Fig. 2). On the other hand, **4** showed only moderate agonist efficacy in a cell-based assay (Table 1). In addition, the plasma exposure level of **4** after oral administration was fairly low, and **4** did not sufficiently show a desired in vivo biological activity in mice.

In this letter, we describe the chemical modification of **4** to enhance the transcriptional activation in a cell-based assay, and to change the physicochemical property with the intent to improve the in vivo pharmacokinetic (PK) behavior, using a structure-guided drug design.

In an effort to find a key to enhance the efficacy in the cell-based assay, the X-ray crystal structure of a human LXRα ligand-binding domain (LBD) in complex with **4** and a peptide derived

* Corresponding authors. Tel.: +81 3 5696 8264; fax: +81 3 5696 4768 (Y.M.); tel.: +81 3 3492 3131; fax: +81 3 5436 8563 (K.T.).
E-mail addresses: matsui.yumi.gk@rdn.daiichisankyo.co.jp (Y. Matsui), tamaki.kazuhiko.s2@daiichisankyo.co.jp (K. Tamaki).

http://dx.doi.org/10.1016/j.bmcl.2015.07.047
0960-894X/

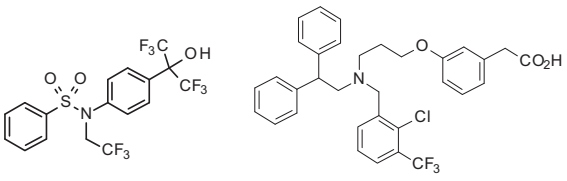

Figure 1. Chemical structures of LXR agonists.

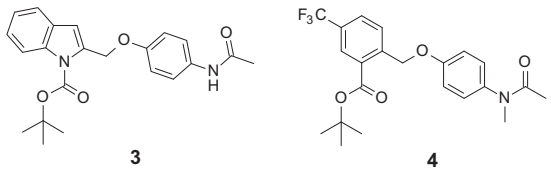

Figure 2. HTS hit compound and its derivative.

Table 1
Profiles of **1**, **2**, **4** and the corresponding C6-hydroxy analog **12**

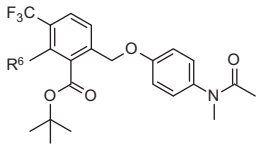

Compound	R^6	FP assay [a] K_i (μM)		CTF assay [b] EC_{50} (μM) (% efficacy)	
		LXRα	LXRβ	LXRα	LXRβ
1		0.23	0.22	0.03 (100)	0.13 (100)
2		0.21	0.16	0.54 (40)	0.10 (72)
4	H	0.87	0.18	0.31 (27)	0.21 (28)
12	OH	0.27	0.17	0.28 (89)	0.26 (76)

[a] FP assay: **1** constantly shows 0.20–0.30 μM of the K_i value toward both LXRs.
[b] CTF assay: efficacy was shown as a relative value based on **1** (100%).

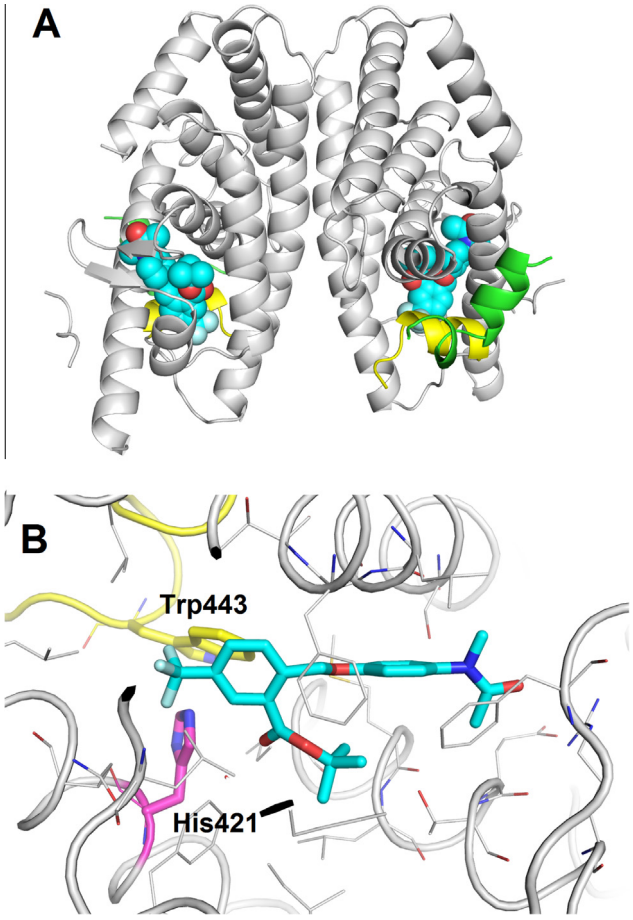

Figure 3. Crystal structure of LXRα-LBD in complex with **4**. (A) The overall structure of LXRα-LBD in complex with **4** and SRC-1 peptide. LXRα-LBD exists as a homodimer in the crystal. LXRα-LBD and SRC-1 peptide are depicted as ribbons, and **4** is shown as a space-filling representation. AF2 region (residues 437–447) of LXRα-LBD are colored in yellow, other parts of LXRα-LBD in gray, and SRC-1 peptide in green. Carbon atoms of compound **4** in cyan, oxygen in red, nitrogen in blue, and fluoride in light blue. (B) Compound **4** in the ligand binding site of LXRα-LBD. Compound **4**, and the side chains of His421 and Trp443 are shown as a stick representation. Other residues included in **4** binding are shown as a line representation. The carbon atoms of His421 and Trp443 are colored in magenta and yellow, respectively. The color scheme of **4** is the same as used in A.

from steroid receptor coactivator-1 (SRC-1 peptide) was determined.[10] LXRα-LBD adopts the three-layered α-helical sandwich structure seen in a typical nuclear receptor LBD fold[11] (Fig. 3A). The C-terminal AF-2 helix is packed against the ligand binding pocket, providing the binding site for SRC-1 peptide. The ligand-binding pocket in which **4** binds is a large cavity, that is, surrounded by Helix-3, Helix-5, Helix-6, Helix-7, Helix-11, and Helix-12. Intermolecular interaction between **4** and the LXRα-LBD are dominated by hydrophobic contacts. As Figure 3B shows, the trifluoromethyl benzyl moiety of **4** binds deep in the pocket, forming van der Waals contacts with the residues Phe257, Thr258, Leu331, His421, Gln424, Leu428, Leu435, and Trp443. The tert-butyl acetate moiety occupies the hydrophobic part which consists of Ile295, Met298, Leu299, Thr302, Phe315, Phe326, Phe335, and Ile339. The right part benzene ring and the *N*-methylacetamide substituent contact Leu260, Ser264, Met298, Glu301, Thr302, Arg305, and Phe315, facing toward the open space surrounded by Helix3, Helix5, and an antiparallel β-sheet. LXRα-LBD (residues from 204 to 447) shares 78% sequence identity with LXRβ-LBD (residues from 218 to 461), and these residues of the LXRα ligand-binding pocket are conserved in LXRβ. Additionally, the overall structure of LXRα-LBD is very similar to that of LXRβ-LBD, as superimposing of the **4** bound LXRα-LBD on the epoxycholesterol bound LXRβ-LBD (PDB ID: 1P8D)[12] exhibits a small root mean square deviation of 0.9 Å over the backbone atoms of 221 residues. Thus, the interactions between **4** and LXRα-LBD would be maintained in LXRβ-LBD with **4**.

Although the published crystal structures of LXRs with agonists have indicated the importance of hydrogen bonding or electrostatic interaction between the agonist and His435 in LXRβ (corresponding to His421 in LXRα) on Helix10/11,[12] our crystal structure has revealed that **4** has only van der Waals interaction with His421 in LXRα-LBD. For example, Williams et al. reported that **1** formed a hydrogen bond with and locked His435 of LXRβ in the position to make an edge to face interaction with Trp457 of LXRβ on the AF2 helix, stabilizing LXRβ-LBD in the active conformation (His-Trp switch).[12] Compound **2** also formed the electrostatic interaction by the trifluoromethyl group with the Nε2 atom of His435 in LXRβ-LBD with 3.3 Å distance (PDB ID: 1PQ6).[13] Unlike these reported agonists, **4** does not have a hydrogen bond or an electrostatic interaction to His421 of LXRα-LBD, but contacts with the Cδ2 atom of His421 by the carbonyl oxygen in the *tert*-butyl benzoate moiety with 3.9 Å distance and by the fluoride atom on the trifluoromethyl group with 4.0 Å distance.

Presuming that the van der Waals interactions of **4** with His421 of LXRα-LBD were not sufficient to lock His421 in the proper

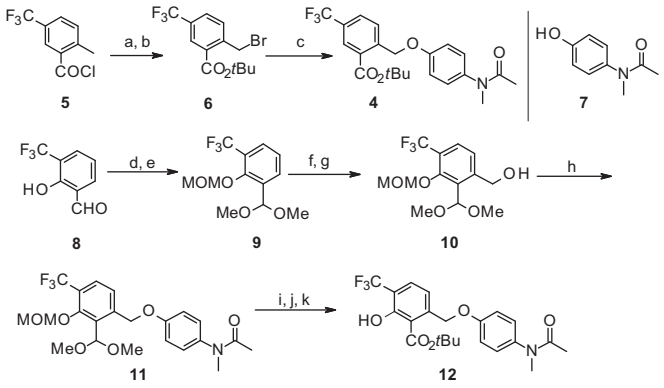

Scheme 1. Reagents and conditions: (a) *t*-BuOK, THF, 0 °C (81%); (b) NBS, AIBN, PhH, reflux (53%); (c) **7**, Cs_2CO_3, DMF (97%); (d) $(MeO)_3CH$, CSA, MeOH, 50 °C; (e) MOMCl, *i*-Pr_2NEt, CH_2Cl_2, 0 °C–rt (93%, 2 steps); (f) *n*-BuLi, TMEDA, Et_2O, −30 °C–rt then DMF at −30 °C; (g) $NaBH_4$, THF–MeOH, 0 °C–rt (52%, 2 steps); (h) **7**, TMAD, *n*-Bu_3P, THF (51%); (i) 4 N HCl–THF, 50 °C; (j) $NaClO_2$, NaH_2PO_4, 2-methyl-2-butene, H_2O–*t*-BuOH; (k) $Me_2NCH(OtBu)_2$, toluene, reflux (40%, 3 steps). TMEDA = *N*,*N*,*N*′,*N*′-tetramethylethylenediamine; TMAD = *N*,*N*,*N*′,*N*′-tetramethylazodicarboxamide.

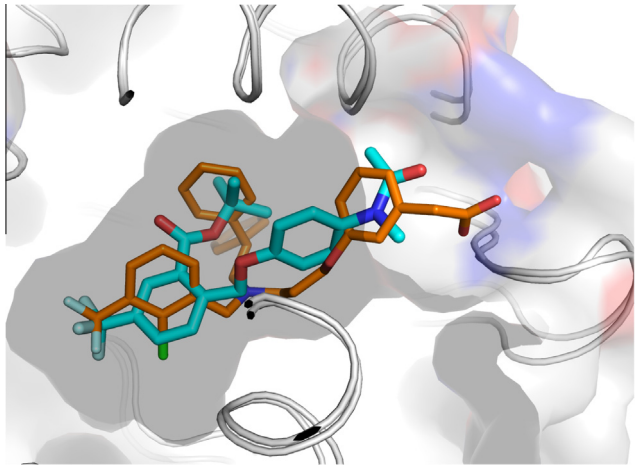

Figure 4. Overlay of **2** in LXRβ-LBD (PDB ID: 1PQ6) on **4** in LXRα-LBD. Compounds **2** and **4** are shown as stick representations, with the carbon atoms colored in orange and cyan, respectively. LXRα-LBD is shown as a surface representation with the color scheme of carbon in gray, nitrogen in blue, and oxygen in red.

position for the His-Trp switch, we tried to modify the compound to form a more robust interaction with His421. Based on the crystal structure, the compound which had the hydroxyl group on the C6 position of the *tert*-butyl benzoate part was predicted to achieve a hydrogen bond with the Nε2 atom of His421.

To test our hypothesis, the C6-hydroxy derivative, **12,** was designed. The synthetic routes of **4** and **12** are shown in Scheme 1. *Tert*-butyl esterification and bromination of acid chloride **5** provided the key intermediate, **6**. By benzylation of phenol **7**[14] with **6**, **4** was prepared. On the other hand, C6-hydroxyl group-installed **12** was synthesized from benzaldehyde **8**.[15] *ortho*-Lithiation of benzaldehyde dimethyl acetal **9**, obtained by the successive protection of phenol and aldehyde of **8**, was followed by a reaction with DMF and reduction by $NaBH_4$ to give another key intermediate, **10**. A Mitsunobu reaction using TMAD[16] of **10** and **7** led to **11**. Deprotection of compound **11** under an acidic condition followed by oxidation and *tert*-butyl esterification provided **12**.

The LXR binding and the efficacy of transcriptional activation of **4** and **12** were evaluated in the fluorescence polarization (FP) assay[17] and the cell transfection (CTF) assay[18], respectively (Table 1). Though the effect of the C6-hydroxyl group installation on K_i in the FP assay and EC_{50} in the CTF assay was small, **12** achieved a three-fold improvement of the efficacy in the CTF assay, as expected.

In parallel to the work to achieve the interaction with His421, we focused on improving the physicochemical properties of our LXR ligand. Because the obtained *tert*-butyl benzoate analogs tended to show poor solubilities (data not shown), we assumed that the low solubility was one of the reasons for low oral absorbability of **4**. Hence we tried to introduce the hydrophilic group to *tert*-butyl benzoate analogs.

A clue for the modification to improve solubility was also obtained from the crystal structures. While searching for a suitable hydrophilic group to introduce, we focused our attention on **2**, which had a terminal carboxyl group in the structure. In the crystal structure of LXRβ-LBD with **2**,[13] the carboxyl group of **2** interacts with Arg319 (Arg305 in LXRα) on Helix5 and Leu330 (Leu316 in LXRα) on the loop between βsheet-1 and βsheet-2. Overlay of the structure of LXRβ-LBD with **2** on that of LXRα-LBD with **4** showed that the *N*-methylacetamide group of **4** occupies a position similar to that of the phenyl ring of the phenyl acetic acid moiety of **2** (Fig. 4). However, **4** does not occupy the space where the terminal

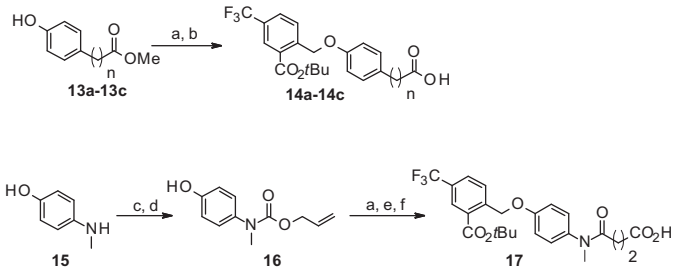

Scheme 2. Reagents and conditions: (a) **6**, K_2CO_3, DMF, rt–0 °C (70–80%); (b) 3 N aq NaOH, THF–MeOH (29–59%); (c) allyl chloroformate, Et_3N, CH_2Cl_2, 0 °C–rt; (d) K_2CO_3, MeOH, rt (74%, 2 steps); (e) $Pd(PPh_3)_4$, pyrrolidine, 1,4,-dioxane-H_2O, rt (85%); (f) succinic anhydride, Et_3N, CH_2Cl_2, 0 °C–rt (68%).

carboxyl methyl group of **2** binds. Thereby, we supposed that the carboxyl group could be fused into **4** by replacing or extending the *N*-methylacetamide group with the tethered carboxyl group. Based on this idea, carboxylic acid analogs were designed and synthesized (Scheme 2).

Compounds **14a**–**c** were prepared from phenols (**13a**–**c**)[19] with the methoxycarbonyl group and **6** in 2 steps (benzylation and hydrolysis). Compound **17** was synthesized from commercially available **15**. Phenol **15** was converted to **16** in 2 steps. Benzylation of **16** with **6**, followed by deprotection of the *N*-alloc group and amidation with succinic anhydride gave **17**.

First, compounds which directly tethered the carboxyl group by several lengths of the linear methylene chain instead of *N*-methylacetamide moiety were tested. As seen from the data in Table 2, the binding affinities of **14a** and **14c** to LXRs were drastically decreased. Nevertheless, **14b** retained a three-fold decreased binding affinity for LXRβ compared to **4**. Compound **17** which contained the extended carboxyl methyl group at the terminal part of **4** also retained moderate binding affinities for LXRs. We suspected that the decreased binding affinities of the carboxylic acid analogs were due to improper interactions of the carboxyl group with the LXRs. Because there was a wide space between the ligand binding pocket and the loop where the carboxyl group was intended to interact, flexible linkers may not have held the carboxyl group at an appropriate location to interact with Leu316 on the loop. Therefore, the benzene ring was selected as a rigid linker to fix the terminal carboxyl group, and biphenyl analogs were designed for the following chemical modification.

Table 2
Binding affinities of the carboxyl group introduced compounds

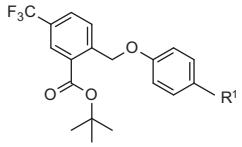

Compound	R^1	FP assay K_i (μM) LXRα	LXRβ
14a	$(CH_2)_3COOH$	N.D.	4.9
14b	$(CH_2)_4COOH$	N.D.	0.63
14c	$(CH_2)_5COOH$	8.6	1.2
17	$N(CH_3)CO(CH_2)_2COOH$	4.0	0.66

N.D.: not determined since a reasonable sigmoid curve could not be obtained.

Table 3
Binding affinities of the carboxyl group introduced biphenyl compounds

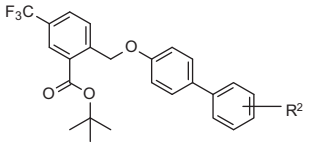

Compound	R^2	FP assay K_i (μM) LXRα	LXRβ
25a	*m*-COOH	6.3	3.4
25b	*p*-COOH	n.a.[a]	n.a.
25c	*m*-CH_2COOH	5.1	0.36
25d	*p*-CH_2COOH	1.0	0.26

[a] n.a.: >10 μM.

The synthesis of biphenyl derivatives (**25a–d**) are shown in Scheme 3. 4-Iodo benzene analog **19**, derived from **18** and **6**, was converted to boronate ester **20**. Compounds **25a–d** were prepared by Suzuki coupling with the appropriate combination of the left hand (**19**, **20**) and the right hand (**21–24**) parts. The following hydrolysis of methyl ester was required for **25b** and **25d**. Toward the synthesis of the C6-hydroxyl group-installed analog, **30a** was prepared by the Suzuki coupling of **26** and **27**. Compound **30b** was also obtained from deprotection of the Suzuki coupling product of **28** and **29**. A Mitsunobu reaction of **30a** with **10** using ADDP,[20] followed by acid hydrolysis led to **31a**. Synthesis of **32a** was carried out by the succeeding O-allylation of **31a**, oxidation to carboxylic acid, *tert*-butyl esterification, deprotection of the allyl group, and hydrolysis of methyl ester. In the same manner, **32b** was synthesized from **30b** and **10** via aldehyde **31b**.

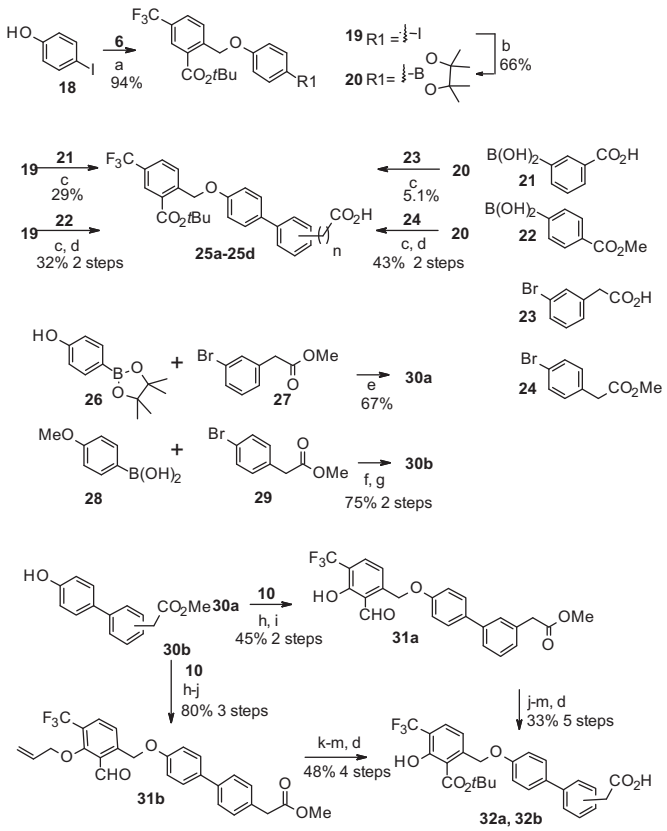

Scheme 3. Reagents and conditions: (a) K_2CO_3, DMF, rt; (b) bis(pinacolato)diboron, $PdCl_2$(dppf), KOAc, DMSO–CH_2Cl_2, 80 °C; (c) $Pd(PPh_3)_4$, K_2CO_3, DMA–H_2O, 90 °C; (d) 3 N aq NaOH, THF–MeOH; (e) $Pd(PPh_3)_4$, K_2CO_3, DMA–H_2O, 110 °C; (f) $Pd(PPh_3)_4$, 1 M aq Na_2CO_3, toluene–EtOAc, reflux; (g) 1 N BCl_3 in CH_2Cl_2, *n*-Bu_4NI, CH_2Cl_2, −78 °C–rt; (h) ADDP, *n*-Bu_3P, THF, rt; (i) *p*-TsOH, acetone, rt; (j) allylbromide, K_2CO_3, DMF, 50 °C; (k) $NaClO_2$, NaH_2PO_4, 2-methyl-2-butene, H_2O-*t*-BuOH, rt; (l) $Me_2NCH(OtBu)_2$ toluene, reflux; (m) $Pd(PPh_3)_4$, pyrrolidine, DMF, rt ADDP = 1,1′-(azodicarbonyl)dipiperidine.

Although the binding affinities of phenyl benzoic acids (**25a** and **25b**) were not attractive, biphenylacetic acids (**25c** and **25d**) maintained similar potency values to **4** in the LXRβ binding. (Table 3).

Based on the structure–activity relationship (SAR) of evaluated compounds, biphenylacetic acid derivatives having the hydroxyl group at the C6-position of the *tert*-butyl benzoate part were designed, expecting to show both improved efficacy of transcriptional activation and oral absorbability. As listed in Table 4, *para*-biphenylacetic acid **32b** showed higher potencies and efficacies than the corresponding *meta*-analog **32a** in the CTF assay. It was also noteworthy that **32b** showed a potent cholesterol efflux activity.[21] Hence **32b** was selected for further in vivo studies. Compound **32b** exhibited a much higher C_{max} and plasma concentration at 6 h after oral administration at a dose of 10 mg/kg than the lead compounds **4** and **12** in mice (Table 5).

To verify the ligand design, the crystal structure of LXRα-LBD in complex with **32b** and SRC-1 peptide was determined.[22] As we have intended, the hydroxyl group of **32b** forms a hydrogen bond to His421 with the length of 3.4 Å (Fig. 5A). Although the location of the carboxyl group of compound **32b** is slightly shifted in LXRα-LBD compared with that of **2** in LXRβ-LBD, one of the carboxyl group oxygens has a hydrogen bond to the main-chain of Leu316 (Fig. 5B), which is comparable to the one seen in **2** with LXRβ-LBD.

Table 4
Profiles of compounds which have both the hydroxyl group and the carboxyl group

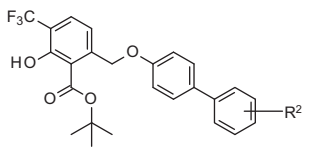

Compound	R^2	CTF assay EC_{50} (μM) (% efficacy) LXRα	LXRβ	Cholesterol efflux assay[a] % efficacy (dose/μM)
32a	*m*-CH_2COOH	1.3 (39)	0.53 (27)	58(1), 3(0.1)
32b	*p*-CH_2COOH	0.51 (79)	0.16(51)	69(1), 57(0.1)

[a] Cholesterol efflux assay: % efficacy was shown at the concentration indicated with parenthesis (μM). The relative value is based on the activity that **1** shows efficacy (100%) at 1 μM concentration.

Table 5
Plasma concentration of the compounds

Compound	Plasma concentration[a]	
	C_{max} (μg/ml)	At 6 h (μg/ml)
4	1.7	1.0
12	1.0	0.67
32b	8.9	5.3

[a] The compounds were orally administered to mice at a dose of 10 mg/kg.

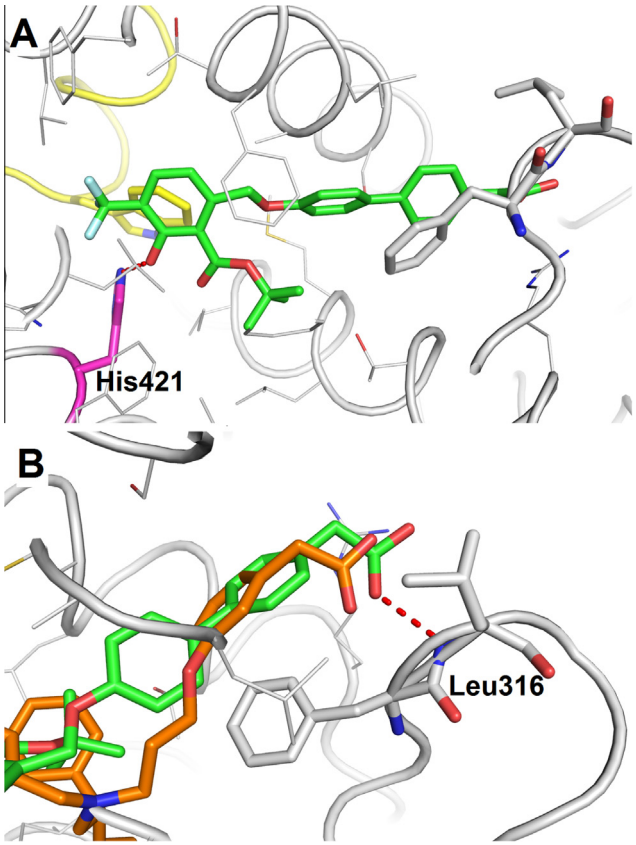

Figure 5. Compound **32b** in the ligand binding site of LXRα-LBD. Compound **32b** is shown as a stick representation with the carbon atoms in green. The color scheme for LXRα-LBD is the same as that used in Figure 3B. Hydrogen bonds are shown as red broken lines. (A) the C6-hydroxyl group is hydrogen bonding to His421. (B) **2** in LXRβ-LBD is overlaid on **32b** in LXRα-LBD. Compound **2** is shown in stick with carbon atoms in orange while LXRβ-LBD is not shown. The carboxyl group of **32b** slightly shifted from that of **2**.

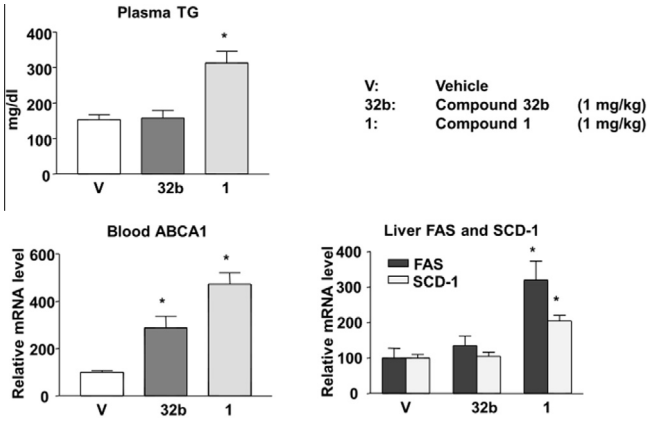

Figure 6. Effect of **32b** and **1** in C57Bl/6 mice. Animals were dosed daily by oral gavage (n = 5/group) for 7 days before measurements. *: p <0.05 as compared with the vehicle group by Dunnett's test.

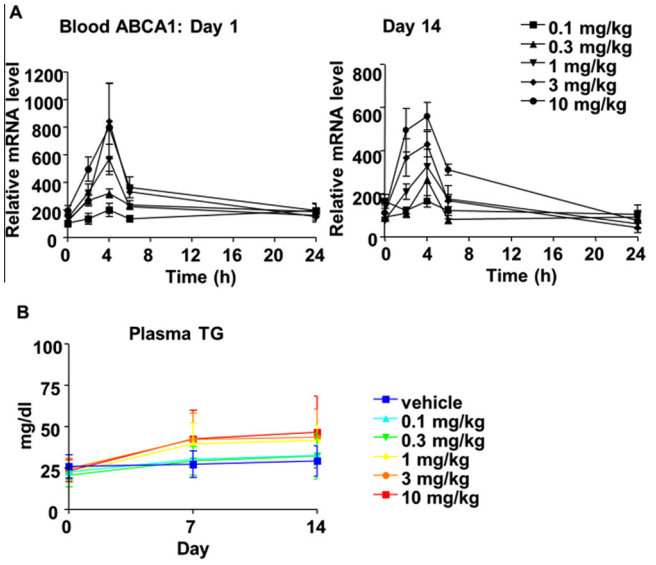

Figure 7. Effect of **32b** in cynomolgus monkeys. Animals were dosed daily by oral gavage (n = 6/group) for 14 days. Results are represented as mean + SE. (A) Line plot of blood ABCA1 mRNA levels on Day 1 and on Day 14. (B) Triglyceride level.

The effects of **32b** and **1** on blood ABCA1, liver FAS and liver SCD-1 mRNA levels, and on plasma TG levels were investigated in C57Bl/6 mice after repeated oral administration at 1 mg/kg for 7 days (Fig. 6). Both **32b** and **1** significantly elevated the blood ABCA1 mRNA levels. On the contrary, **32b** did not affect the liver FAS mRNA levels, liver SCD-1 mRNA levels, nor plasma TG levels while **1** elevated them. To further investigate the pharmacological property, **32b** (0, 0.1, 0.3, 1, 3 or 10 mg/kg) was orally administered to cynomolgus monkeys for 14 days. Treatment with **32b** significantly elevated blood ABCA1 mRNA expression in a dose dependent manner on both Day 1 and Day 14 (Fig. 7A). Importantly, **32b** did not affect plasma TG after repeated dosing as well as single dosing (Fig. 7B).

To elucidate why **32b** had the wide window between ABCA1 and TG elevation, a fluorescence resonance energy transfer (FRET) assay was carried out using LXRs and synthetic peptides from transcriptional cofactors.[23] Two cofactors, peroxisome-proliferator-activated receptor gamma coactivator 1α (PGC1α) and activating signal cointegrator 2 (ASC2), were identified as the potential determinants. PGC1α has been reported as a potent transcriptional coactivator for LXRα, and potentiates its transcriptional activity upon the SREBP-1c gene promoter.[24] ASC2 has also been identified as a physiologically important transcriptional coactivator of LXRα in regard to lipid metabolism in the liver.[25] The effect of **32b** for LXRα on PGC1α or ASC2 recruitment was less efficacious than that of **1**, while both **32b** and **1** induced the recruitment of PGC1α or ASC2 to LXRβ to almost the same extent (Fig. 8). This characteristic cofactor recruitment property of **32b** might be one of the reasons why **32b** has the favorable pharmacological property of ABCA1 expression without FA expression, SCD1 expression, nor TG elevation.

In summary, a SAR study on a series of *tert*-butyl benzoate analogs was performed to obtain a potent LXR agonist. The **4** bound LXRα-LBD structure, along with the **2** bound LXRβ-LBD structure, led us to introduce the hydroxyl group at the C6-position of the *tert*-butyl benzoate core to enhance the efficacy in the cell-based reporter assay, and to introduce the carboxyl group tethered by

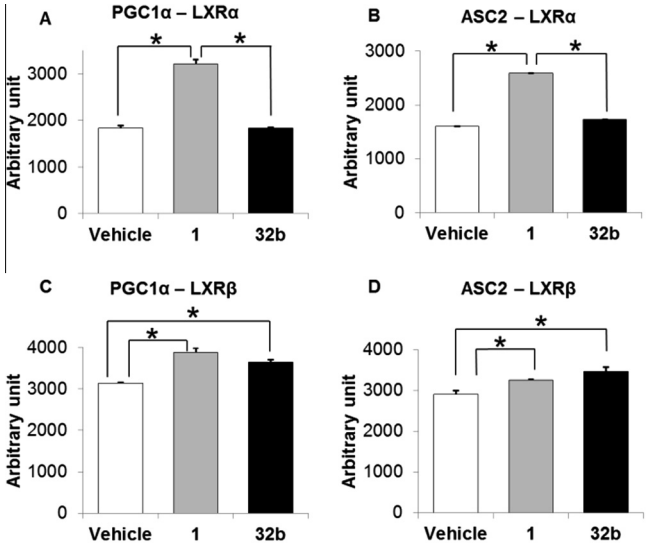

Figure 8. Effects of **32b** and **1** on cofactor recruitment to LXRs. Effects of **32b** and **1** on PGC1α or ASC2 recruitment to LXR were examined by a fluorescence resonance energy transfer assay. $^{*}p<0.05$, as compared with the vehicle control group and **1** group or **32b** group and **1** group using Student's *t*-test. The data are represented as mean + SE ($n = 4$). (A) PGC1α to LXRα. (B) ASC2 to LXRα. (C) PGC1α to LXRβ. (D) ASC2 to LXRβ.

biphenyl at one terminal to improve the oral absorbability. The obtained compound, **32b**, exhibited a potent LXR agonistic activity in a cell-based assay, showed good exposure of post-oral administration, and induced blood ABCA1 mRNA expression without affecting the plasma TG levels in both mice and cynomolgus monkeys.

Acknowledgments

We thank Yasuko Kono for her evaluation of the FP assay, Ayano Ogawa-Hiroshima for her evaluation of the cholesterol efflux assay, Tomoko Takayama for the protein production, and Rie Nakagomi-Hagihara for the pharmacokinetic study. The HTS screen was carried out at X-Ceptor (now Exelixis). The initial LXRα-LBD crystallization protocol was developed at Syrrx (now Takeda California) and further optimized at Sankyo (now Daiichi Sankyo RD Novare).

Supplementary data

Supplementary data associated with this article can be found, in the online version, at http://dx.doi.org/10.1016/j.bmcl.2015.07.047. These data include MOL files and InChiKeys of the most important compounds described in this article.

References and notes

1. (a) Willy, P. J.; Umesono, K.; Ong, E. S.; Evans, R. M.; Heyman, R. A.; Mangelsdorf, D. J. *Genes Dev.* **1995**, *1033*, 9; (b) Jaye, M. *Curr. Opin. Investig. Drugs.* **2003**, *1053*, 4.
2. Laffitte, B. A.; Repa, J. J.; Joseph, S. B.; Wilpitz, D. C.; Kast, H. R.; Mangelsdorf, D. J.; Tontonoz, P. *Proc. Natl. Acad. Sci. U.S.A.* **2001**, *98*, 507.
3. (a) Venkateswaran, A.; Laffitte, B. A.; Joseph, S. B.; Mak, P. A.; Wilpitz, D. C.; Edwards, P. A.; Tontonoz, P. *Proc. Natl. Acad. Sci. U.S.A.* **2000**, *97*, 12097; (b) Wang, N.; Lan, D.; Chen, W.; Matsuura, F.; Tall, A. R. *Proc. Natl. Acad. Sci. U.S.A.* **2004**, *101*, 9774; (c) Nakamura, K.; Kennedy, M. A.; Baldán, Á.; Bojanic, D. D.; Lyons, K.; Edwards, P. A. *J. Biol. Chem.* **2004**, *279*, 45980; (d) Baldán, Á.; Bojanic, D. D.; Edwars, P. A. *J. Lipid Res.* **2009**, *50*, S80.
4. Joseph, S. B.; Tontonoz, P. *Curr. Opin. Pharmacol.* **2003**, *3*, 192.
5. For reviews on the therapeutic utilities of LXR modulators, see (a) Collins, J. L. *Curr. Opin. Drug Discov. Dev.* **2004**, *7*, 692; (b) Bradley, M. N.; Tontonoz, P. *Drug Discov. Today: Therapeutic Strategies* **2005**, *2*, 97; (c) Geyeregger, R.; Zeyda, M.; Stulnig, T. M. *Cell. Mol. Life Sci.* **2006**, *63*, 524; (d) Bradley, M. N.; Hong, C.; Chen, M.; Joseph, S. B.; Wilpitz, D. C.; Wang, X.; Lusis, A. J.; Collins, A.; Hseuh, W. A.; Collins, J. L.; Tangirala, R. K.; Tontonoz, P. *J. Clin. Invest.* **2007**, *117*, 2337; (e) Gabbi, C.; Warner, M.; Gustafsson, J.-A. *Mol. Endocrinol.* **2009**, *23*, 129.
6. (a) Repa, J. J.; Turley, S. D.; Lobaccaro, J.-M. A.; Medina, J.; Li, L.; Lustig, K.; Shan, B.; Heyman, R. A.; Dietschy, J. M.; Mangelsdorf, D. J. *Science* **2000**, *289*, 1524; (b) Terasaka, N.; Hiroshima, A.; Koieyama, T.; Ubukata, N.; Morikawa, Y.; Nakai, D.; Inaba, T. *FEBS Lett.* **2003**, *536*, 6.
7. (a) Collins, J. L.; Fivush, A. M.; Watson, M. A.; Galardi, C. M.; Lewis, M. C.; Moore, L. B.; Parks, D. J.; Wilson, J. G.; Tippin, T. K.; Binz, J. G.; Plunket, K. D.; Morgan, D. G.; Beaudet, E. J.; Whitney, K. D.; Kliewer, S. A.; Willson, T. M. *J. Med. Chem.* **1963**, *2002*, 45; (b) Joseph, S. B.; McKilligin, E.; Pei, L.; Watson, M. A.; Collins, A. R.; Laffitte, B. A.; Chen, M.; Noh, G.; Goodman, J.; Hagger, G. N.; Tran, J.; Tippin, T. K.; Wang, X.; Lusis, A. J.; Hsueh, W. A.; Law, R. E.; Collins, J. L.; Willson, T. M.; Tontonoz, P. *Proc. Natl. Acad. Sci. U.S.A.* **2002**, *99*, 7604.
8. Schultz, J. R.; Tu, H.; Luk, A.; Repa, J. J.; Medina, J. C.; Li, L.; Schwendner, S.; Wang, S.; Thoolen, M.; Mangelsdorf, D. J.; Lustig, K. D.; Shan, B. *Genes Dev.* **2000**, *14*, 2831.
9. Shimomura, I.; Shimano, H.; Korn, B. S.; Bashmakov, Y.; Horton, J. D. *J. Biol. Chem.* **1998**, *273*, 35299.
10. Crystals were obtained by mixing equal volumes of the precipitant solution (8–18% (w/v) polyethylene glycol 2000 monomethyl ether, 0.18 M ammonium sulfate, and 0.1 M Tris–HCl (pH 7.5)) and the mixture of LXRα-LBD, the compound, and SRC-1 peptide (20 mM Tris–HCl (pH 8.0), 50 mM sodium chloride, 0.1 mM EDTA, and 1 mM DL-dithiothreitol). The atomic coordinates for the crystal structure of LXRα-LBD in complex with **4** and SRC-1 peptide were deposited in the Protein Data Bank, with the PDB accession code, 5AVI.
11. Weatherman, R. V.; Fletterick, R. J.; Scanlan, T. S. *Annu. Rev. Biochem.* **1999**, *68*, 559.
12. Williams, S.; Bledsoe, R. K.; Collins, J. L.; Boggs, S.; Lambert, M. H.; Miller, A. B.; Moore, J.; McKee, D. D.; Moore, L.; Nichols, J.; Parks, D.; Watson, M.; Wisely, B.; Willson, T. M. *J. Biol. Chem.* **2003**, *278*, 27138.
13. Färnegårdh, M.; Bonn, T.; Sun, S.; Ljunggren, J.; Ahola, H.; Wilhelmsson, A.; Gustafsson, J. A.; Carlquist, M. *J. Biol. Chem.* **2003**, *278*, 38821.
14. Fernando, C. R.; Calder, I. C.; Ham, K. N. *J. Med. Chem.* **1980**, *23*, 1153.
15. Daly, A. M.; Gilheany, D. G. *Tetrahedron: Asymmetry* **2003**, *14*, 127.
16. Tsunoda, T.; Otsuka, J.; Yamamiya, Y.; Itô, S. *Chem. Lett.* **1994**, *23*, 539.
17. Fluorescence polarization (FP) assay: assay buffer was composed of 10 mM HEPES (pH 7.0), 0.1 mM EDTA 3Na, 10 mM DTT, 20% (v/v) Ultrapure BGG 5 mg/ml (Invitrogen Co.), 0.5 nM fluorescein isothiocyanate (FITC)-labeled T0901317 and 1 μM His-LXRα/FLAG-RXRα or 1 μM His-LXRβ/FLAG-RXRα. FP assay employed 38 μl of buffer with 2 μl of test compound in DMSO, which was placed at room temperature overnight before measurement.
18. Cell transfection (CTF) assay: The African green monkey kidney-derived cell line and CV-1 cells were cultured in DMEM supplemented with 10% charcoal/dextran-treated FBS (HyClone), 1% penicillin-streptomycin, 1% Gluta Max-1 (Invitrogen Co.), and 1 mM sodium pyruvate (Invitrogen Co.) at 37 °C. On the day before transfection, the CV-1 cells were seeded in 96-well assay plates at 2.0×10^4 cells/well and placed for 20 h. Expression plasmid pcDNA-hLXRα or pcDNA-hLXRβ and luciferase reporter plasmid pTAL-LXRE including LXR response element (ref. Willy P.J. et al.: *Genes Dev.* **1995**, *9*, 1033.) were transfected with Lipofectamine Reagent (Invitrogen Co.). After 3 h, 70 μl of the DMEM medium was added. Then, DMSO solutions of the test compounds or DMSO alone (for the control) were added. The cells were further incubated for about 20 h .The luciferase assay was performed using Luciferase Assay Reagent (Promega Co.). The luminescence intensity in each well was measured using a luminescence plate reader (Analyst HT, Molecular Devices). The luminescence intensity was represented as counts per second (CPS). The luminescence intensity data were analyzed by the Sigmoid E_{max} model.
19. (a) Hazeldine, S. T.; Polin, L.; Kushner, J.; White, K.; Corbett, T. H.; Horwitz, J. P. *Bioorg. Med. Chem.* **2005**, *13*, 3910; (b) Yi, C.-S.; Martinelli, L. C.; Blanton, C.; DeWitt, Jr. *J. Org. Chem.* **1978**, *43*, 405; (c) Chu, L.; Hutchins, J. E.; Weber, A. E.; Lo, J.-L.; Yang, Y.-T.; Cheng, K.; Smith, R. G.; Fisher, M. H.; Wyvratt, M. J.; Goulet, M. T. *Bioorg. Med. Chem. Lett.* **2001**, *11*, 509.
20. Tsunoda, T.; Yamamiya, Y.; Itô, S. *Tetrahedron Lett.* **1993**, *34*, 1639.
21. Cholesterol efflux assay: RAW264.7 cells were seeded in a 96-well plate and cultured in DMEM supplemented with 1% FBS and 1% penicillin-streptomycin, including 0.2 μCi/ml [4-^{14}C]-cholesterol (PerkinElmer, Inc.) for 2 days. After washing the cells with 0.2% albumin bovine serum (BSA, Sigma–Aldrich Co.)/PBS, 100 μl/well of apoAI(−) medium or apoAI(+) medium (DMEM including 10 μg/ml apoAI (Biogenesis)) was added. The test compounds (final concentrations: 0.01, 0.1, and 1 μM) and DMSO alone were added and the cells were further incubated for about 24 h. Then, 75 μl of the medium in each well was transferred to a Luma Plate (PerkinElmer, Inc.) and dried in the draft chamber. The cells were washed with PBS and 250 μl of MICROSCINT 20 (PerkinElmer, Inc.) was added, and then incubated at room temperature overnight. Cellular (assay plate) and medium (Luma Plate) radioactivities (cpm) were measured by TOPCOUNT (B991201, Packard). ApoAI-dependent cholesterol efflux (%) was calculated according to the following formula: Cholesterol efflux (%) = counts in medium (cpm)/[counts in medium (cpm) + counts in cells (cpm)] * 100 ApoAI-dependent cholesterol efflux (%) = cholesterol efflux in the case of apoAI(+) medium (%) − mean cholesterol efflux in the case of apoAI(−) medium (%).
22. The atomic coordinates for the crystal structure of LXRα-LBD in complex with **32b** and SRC-1 peptide were deposited in the Protein Data Bank, with the PDB accession code, 5AVL.
23. Recruitment of the PGC1α peptide (residues 130–154) and ASC2 peptide (residues 1481–1510) as transcriptional cofactors to His-LXRα & Flag-RXRα

protein and His-LXRβ & Flag-RXRα protein were investigated with a FRET assay, based on the non-radiative energy transfer of the long-lived emission from the europium cryptate donor t the cross-linked allophycocyanin (XL665) acceptor. Two microliters of 1 mM compound or DMSO alone (for the DMSO control) was pipetted into the wells of a 384 well plate ($n = 4$). Then, 8 μl of the His-LXRα & Flag-RXRα mixture solution or the His-LXRβ & Flag-RXRα mixture solution was added to each well and the contents of the wells were mixed using a plate shaker. After 60 min of incubation at room temperature, 10 μl of the PGC1α mixture solution or the ASC2 mixture solution was added to the individual wells and the contents of the wells were mixed using the plate shaker. After one night of incubation at 4 °C, the emission of fluorescence excited by a laser at 320 nm was measured at wavelengths of 620 nm (B-count, cpm) and 665 nm (A-count, cpm) using a fluorescence plate reader (WALLAC EnVision, PerkinElmer, Inc.).

24. (a) Oberkofler, H.; Schraml, E.; Krempler, F.; Patsch, W. *Biochem. J.* **2003**, *371*, 89; (b) Oberkofler, H.; Schraml, E.; Krempler, F.; Patsch, W. *Biochem. J.* **2004**, *381*, 357.
25. Kim, S. W.; Park, K.; Kwak, E.; Choi, E.; Lee, S.; Ham, J.; Kang, H.; Kim, J. M.; Hwang, S. Y.; Kong, Y. Y.; Lee, K.; Lee, J. W. *Mol. Cell. Biol.* **2003**, *23*, 3583.